

Phase stability of lithium azide at pressures up to 60 GPa

This article has been downloaded from IOPscience. Please scroll down to see the full text article.

2009 J. Phys.: Condens. Matter 21 195404

(<http://iopscience.iop.org/0953-8984/21/19/195404>)

View [the table of contents for this issue](#), or go to the [journal homepage](#) for more

Download details:

IP Address: 129.252.86.83

The article was downloaded on 29/05/2010 at 19:33

Please note that [terms and conditions apply](#).

Phase stability of lithium azide at pressures up to 60 GPa

S A Medvedev^{1,2}, I A Trojan¹, M I Eremets¹, T Palasyuk^{1,3},
T M Klapötke⁴ and J Evers⁴

¹ Max-Planck-Institute for Chemistry, Postfach 3060, D-55020 Mainz, Germany

² Institute für Anorganische und Analytische Chemie, Johannes Gutenberg-Universität, D-55099 Mainz, Germany

³ Institute of Physical Chemistry, Polish Academy of Sciences, Kasprzaka 44/52, 01-224, Warsaw, Poland

⁴ Energetic Materials Research, Ludwig-Maximilian University Munich (LMU), Butenandtstrasse 5-13(D), D-81377 Munich, Germany

E-mail: medvedev@mpch-mainz.mpg.de

Received 14 January 2009, in final form 24 March 2009

Published 16 April 2009

Online at stacks.iop.org/JPhysCM/21/195404

Abstract

We studied lithium azide (LiN_3) by x-ray diffraction and Raman spectroscopy at hydrostatic compression up to pressures above 60 GPa at room temperature. The results of x-ray diffraction analyses reveal the stability of the ambient-pressure $C2/m$ crystal structure up to the highest pressure. The pressure dependence of librational modes provides evidence for an order–disorder transition at low pressures (below 3 GPa), similar to the transition observed previously at low temperatures. The observed structure stability indicates that this transition is not associated with structural changes. The phase stability of LiN_3 is in contrast to that of sodium azide (which is isostructural at ambient pressure), for which a set of phase transitions has been reported at pressures below 50 GPa.

1. Introduction

Metal azides have attracted considerable interest [1] for several reasons; for example, upon being subjected to external influences (heat, irradiation, etc), they develop instability, resulting in decomposition into nitrogen and metal accompanied by burning (ignition and combustion in the case of alkali azides) or explosion (heavy metal azides). This property has resulted in the practical application of azides as a source of chemically pure nitrogen, as initial explosives, and even as photographic materials at low temperature. To understand the decomposition mechanism, several studies have investigated the electronic structure of metal azides [2–6].

From a more general viewpoint, metal azides are of interest as model systems for studying the main regularities of chemical reactions in solids with complex chemical bonding [1]. The alkali azides that possess a linear molecular anion provide a new challenge for calculations of crystal structure, lattice dynamics and electronic structure, representing the next-level model of ionic compounds beyond the extensively studied (as model systems) alkali halides. In this respect, experimental high-pressure studies of azides are

believed to help in such calculations by providing a large amount of valuable data.

An important aspect of studies of azides at high pressure is the prospect of their use as a precursor in the formation of polymeric nitrogen—the ultimate example of a high energy density material [7, 8]. Recent studies have reported the transformation of sodium azide (NaN_3) to a non-molecular nitrogen state with an amorphous-like structure when compressed to high pressures [9, 10]. In this respect, a comparison of the high-pressure behaviour of these substances (which are isostructural at ambient pressure) would enable an understanding of the mechanism of pressure-induced rearrangement of azide ions and phase transitions that might result in the formation of polymeric nitrogen.

Under ambient conditions, lithium azide (LiN_3) crystallizes in a monoclinic lattice with $C2/m$ symmetry and lattice parameters $a = 5.627 \text{ \AA}$, $b = 3.319 \text{ \AA}$, $c = 4.979 \text{ \AA}$ and $\beta = 107.4^\circ$; it possesses two formula units per unit cell (shown schematically in the inset in figure 1) [11] and is isostructural to a low-temperature phase of sodium azide in all respects. Azide ion groups form layers separated by layers of Li ions. The

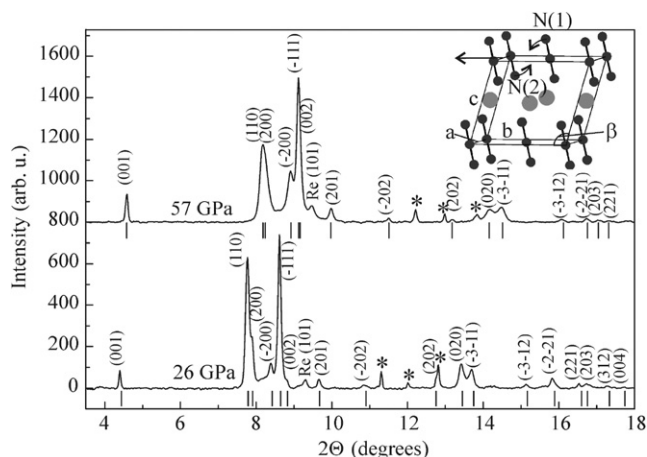


Figure 1. Diffraction patterns of LiN_3 at 26 and 57 GPa at room temperature. The patterns are assigned to the $C2/m$ structure shown schematically in the inset. The tick marks below the patterns show the calculated reflection positions. The Pt standard lies outside the area from which the presented patterns were collected (beam spot diameter $\approx 5 \mu\text{m}$) and therefore does not contribute to the patterns. Peaks marked with asterisks are due to unidentified contaminants in the sample.

anion axes are parallel to each other and tilted by about 11.5° within the layers in which they are stacked.

At ambient pressure, LiN_3 has been studied previously by x-ray diffraction [11] and Raman spectroscopy in the temperature region 100–300 K [12]; no high-pressure experimental data are available. Here we present the results of experimental studies of LiN_3 by x-ray diffraction and Raman spectroscopy under hydrostatic compression up to pressures of 62 GPa at room temperature.

2. Experimental methods

LiN_3 was prepared according to the literature [13, 14]. A total of 1.30 g of NaN_3 and 1.41 g of $\text{Li}_2\text{SO}_4 \cdot \text{H}_2\text{O}$ was dissolved in 7 ml of water. To this solution, 35 ml of ethanol was added. After 10 min, the reaction mixture was filtered and the precipitate (Na and Li sulfates) was washed with ethanol. The filtrate and wash liquid were combined and evaporated to near dryness using a rotary evaporator. Final drying was carried out at 80°C in an oven under ambient pressure. The yield of LiN_3 was 1.02–1.04 g.

The samples were loaded in a diamond anvil cell with an Re gasket. The diamond anvils had flat culets of diameter $350 \mu\text{m}$. To avoid sample contamination arising from the high hygroscopicity of LiN_3 , samples were loaded in a glove box in an atmosphere of pure nitrogen, containing <0.1 ppm of oxygen and water. We used synthetic diamonds with low intrinsic luminescence and helium as a pressure medium, thereby yielding high-quality Raman spectra to the highest pressures. An HeNe laser with a power of 25 mW was used for the excitation of Raman spectra. The laser radiation did not damage the samples and did not excite any appreciable luminescence. Raman spectra were recorded with a single imaging spectrometer HR460 (focal length 460 mm) equipped

with a $900 \text{ grooves mm}^{-1}$ grating, giving a resolution of $\sim 1 \text{ cm}^{-1}$. The spectrometer was equipped with notch filters and a cooled charge-coupled device. Raman scattering was calibrated using Ne lines with an uncertainty of $\pm 1 \text{ cm}^{-1}$. Angle-dispersive x-ray diffraction studies were performed at station 13-IDD at the Advanced Photon Source ($\lambda = 0.3344 \text{ \AA}$). Pressure was measured by the Raman shift of the high-frequency edge of the stressed diamonds [15] (with correction for the hydrostatic medium [16]) in the spectroscopic studies, and by a chip of Pt foil placed in the anvil cell with the sample for x-ray studies. The accuracy of pressure determination from the Raman shift of the stressed diamond anvil using the calibrating equation from [16] is estimated as ± 0.3 GPa, while the accuracy of pressure determination in our x-ray studies from the equation of state of Pt [17] is estimated as ± 0.4 GPa. The x-ray diffraction patterns were taken at the pressure load run while Raman studies were performed both at pressure load and upload runs with reproducible results.

3. Results and discussion

The x-ray diffraction pattern of LiN_3 collected at 26 GPa and room temperature is assigned to the $C2/m$ structure, similar to the structure observed under ambient conditions, with lattice parameters $a = 4.92 \text{ \AA}$, $b = 2.85 \text{ \AA}$ and $c = 4.38 \text{ \AA}$, and monoclinic angle $\beta = 99.4^\circ$ (figure 1). With further compression at room temperature up to pressures above 60 GPa, the diffraction pattern shows little change (figure 1), indicating that the monoclinic structure is retained.

Figure 2 shows the pressure dependences of the cell volume, lattice constants and monoclinic angle β . The unit cell of LiN_3 is highly compressible: at 62 GPa its volume represents just $\approx 58\%$ of the initial volume. The fit of the experimental data of the unit cell volume to the third-order Birch–Murnaghan equation of state (solid line in figure 2(a)) yields a bulk modulus value of $B_0 = 19.1 \pm 1.4$ GPa and a first pressure derivative of $B'_0 = 7.3 \pm 0.5$. Thus, the compressibility of LiN_3 is similar to that of alkali halides (e.g. NaCl, which yields $B_0 = 23.84$ GPa and $B'_0 = 5.35$ [18]).

The pressure dependence of the lattice constants of LiN_3 exhibits a slight anisotropy, as shown in the inset in figure 2(b). The smallest lattice deformation is observed along the c axis. Together with the decreasing monoclinic angle β (figure 2(c)), this deformation leads to only a slight change in the interlayer distance (star symbols in figure 2(b)); deformation is concentrated within the basal ab plane. The strongest deformation occurs along the b axis, as expected given that the azide ions lie in the monoclinic ac planes oriented perpendicular to the b axis. The anisotropy of compressibility within the basal plane leads to a continuous increase in the value of a/b , attaining 1.73438 ($\approx \sqrt{3}$) at 62 GPa; consequently, the centres of azide ions within the basal planes form a regular hexagonal lattice at this pressure.

The principal structural change that occurs with increasing pressure is the shear of layers, as indicated by a large decrease in the monoclinic angle β (figure 2(c)). This effect is especially significant at pressures below 20 GPa: the change

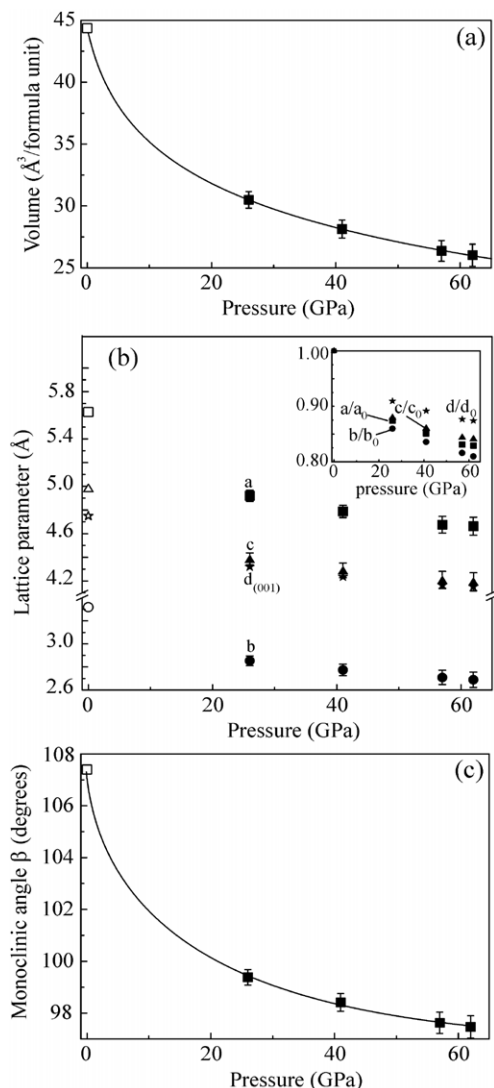


Figure 2. Pressure dependence of the unit cell volume (a), lattice parameters and interlayer distance $d_{(001)}$ (b), and monoclinic angle β (c). Lattice parameters were refined with zero shift correction using the *FullProf* software package. Open symbols represent values at ambient pressure (from [11]). The solid line in (a) shows the fit of the data to the Birch–Murnaghan equation of state with $B_0 = 19.1$ GPa and $B'_0 = 7.3$. The solid line in (c) is a visual guide only. The inset in (b) shows changes in lattice parameters normalized to values at ambient pressure.

in monoclinic angle is close to $\approx 8^\circ$ at low pressures, but only $\approx 2^\circ$ at 26–62 GPa. This interlayer shear is associated with a disproportionately large tilt of the azide ions within the monoclinic plane⁵. The occurrence of these two discrete

⁵ Unfortunately, the tilting angle could not be determined directly from our data because of a significant preferred orientation in the sample; in addition, the number of observed reflections was insufficient to perform a full-profile Rietveld refinement of the structure. The proportionality between the shear of the layers and the tilt angle of the anions can be deduced from the values at the α – β phase transitions in sodium azide: the shear of layers is 4.8° , while the associated tilt of anions is 12.3° [11]. A similar transition in the LiN₃ was not reported and occurs apparently at elevated temperatures. However, the very close values of monoclinic angles in the $C2/m$ structure of LiN₃ and NaN₃ (107.4° and 108.43° , respectively) and anion tilt (11.5° and 12.3° , respectively) indicate the similar relation between the shear of layers and tilts of the azide ions for the LiN₃.

regions of pressure dependence of monoclinic angle (shear) may reflect a change in the nature of interaction between adjusting azide anions. The change in tilt angle at pressures below 20 GPa results in a more energetically favourable arrangement of azide ions, as end atoms with a partial negative charge [19] become closer to the partially positively charged central N atom of the adjacent N₃[−] anion. On further compression (above 20 GPa), the tilting of anions leads to a reduction in the distance between the end atoms N(1) of one anion and N(2) of the adjacent anion (inset in figure 1), resulting in turn in an increase in the contribution of the repulsive component of the overall interaction between the atoms. Hence, the observed interlayer shear becomes less sensitive to increasing pressure at pressures above 20 GPa; in other words, the energy of repulsive interaction partially offsets the effect of pressure.

Of note, our x-ray diffraction data reveal that the monoclinic structure of LiN₃ remains stable up to at least 62 GPa pressure, in contrast to isostructural NaN₃, for which previous spectroscopic studies have reported a set of pressure-induced phase transitions in the pressure range below 60 GPa [9, 10]. Our Raman studies of LiN₃ confirm its distinctive phase stability and provide further details of the rearrangement of azide ions under pressure.

According to group theory, the monoclinic phase of LiN₃ has three Raman active modes: one internal symmetric stretching of the azide ion and two librational modes of A_g and B_g symmetry. All three modes have been observed experimentally at ambient pressure [12] and no additional modes have been observed at compression up to 62 GPa (figure 3). We observed no significant inhomogeneous broadening or decrease in intensity of the vibron of the azide ion (figure 3(b)), indicating no weakening of interatomic bonds in the ion. The frequencies of all observed modes shifted smoothly (without any discontinuities) to higher energy with increasing pressure (figures 3(c) and (d)), indicating, as expected, increasing interaction between the nitrogen atoms. The Raman spectra show no indication of structural transformations, thereby demonstrating the stability of the monoclinic $C2/m$ phase.

Further information on the behaviour of azide ions under compression can be gained from a study of libration modes. At ambient pressure and room temperature, the A_g and B_g librational modes are accidentally degenerated; this degeneration is eliminated at lower temperature [12]. The splitting of libron modes indicates an order–disorder transition at low temperature [12]. It remains unclear whether this transition is associated with changes in crystal structure at low temperature. The present results show that an increase in pressure also eliminates the degeneration of libron modes, and already at the lowest experimental pressure of 3 GPa the splitting is ≈ 50 cm^{−1} (figure 3(d)). Such a high value of the mode-splitting (by cooling down to 100 K at ambient pressure this value reaches ≈ 20 cm^{−1} only [12]) indicates that the order–disorder transitions occurs most likely at low pressures of several kbars only. Because the $C2/m$ structure has been demonstrated to be stable at high pressure, the order–disorder transition is not considered to be associated with structural

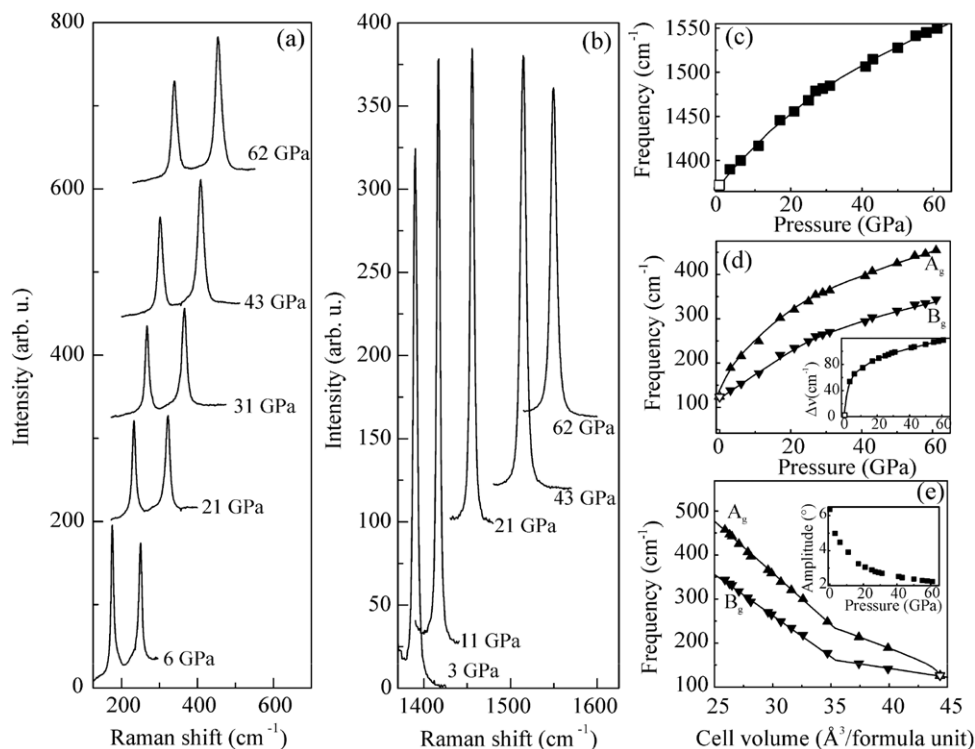


Figure 3. Raman spectra of librons (a) and azide ionic vibron (b) of LiN₃ at different pressures at room temperature. (c) Dependence of vibron frequency on pressure. (d) Dependence of libron modes on pressure and mode frequency splitting versus pressure (inset). (e) Dependence of libron mode on cell volume. The inset shows the dependence on pressure of the angular displacement from equilibrium. Open symbols in panels (c)–(e) represent values at ambient pressure and room temperature from [12]. Solid lines in panels (c)–(e) are visual guides only.

changes. The orientational disorder at ambient conditions is most likely to be dynamic in nature [12] manifested in anion jumps (or hindered gyration) between potential minima located in the space between the cations’ in which the end atom of the azide anion comes closer to one of the three nearest cations.

As pressure increases the mode-splitting shows a strong increase (see the inset in figure 3(d)) because of a significantly larger pressure coefficient for the high-frequency A_g compared to that for the B_g mode. This difference in mode behaviour cannot be explained solely in terms of the slight anisotropy in pressure-induced deformation of the basal plane (see the inset in figure 2(b)): it is most likely caused by anisotropy of the interaction among the tilted anions.

It is instructive to consider the dependence of libron frequency on cell volume. The trend in frequency dependence of both modes on cell volume shows a clear change in slope at a pressure of ≈15–20 GPa (figure 3(e)). Below this pressure, the increase in frequency is determined by pressure-enhanced interaction of the increasingly ordered tilting of anions. At higher pressures, the repulsion between the end atoms of adjacent anions causes significant hardening of the interionic potential, resulting in an increasing dependence of librational frequency on volume.

The libron frequencies observed in Raman scattering enable estimates of the amplitude of torsional motion of anions in the crystal. For a crystal with linear molecules on centrosymmetric sites, the average mean square amplitude is

given by

$$\langle \theta^2 \rangle = (h/8\pi^2 n I) \sum_j (g_j / \nu_j) \coth(h\nu_j / 2kT),$$

where θ is the angular displacement from equilibrium in radians; I is the moment of inertia of the molecule; g_j and ν_j are the degeneracy and frequency of the j th libration, respectively; j is summed over all the zone-centre librational frequencies; and n is the sum of g_j values [20, 21].

The degree of pressure dependence of the angular amplitude (inset in figure 3(e)) shows a sharp drop at pressures below 20 GPa, indicating the strong hindering of libration motion by increasing repulsive interaction of the negatively charged end atoms of adjacent anions. Thus, the librational motion becomes strongly hindered at pressures of about 20 GPa. Given that the thermodynamic functions of crystals are strongly dependent on librational frequencies, the anomalies of the thermodynamic parameters would be expected at this pressure.

In conclusion, x-ray diffraction and Raman spectroscopy studies demonstrate the stability of the C2/m structure of lithium azide at hydrostatic compression up to pressures above 60 GPa. The shear of layers and associated increase in tilt of azide anions leads to the enhanced repulsion of the end atoms of adjacent anions. It might be expected that, at higher pressures, the parallel arrangement of azide ions would become energetically unfavourable, and that anions would be ‘squeezed’ out of the monoclinic plane towards forming a T-like arrangement that is more favourable for linear azide

anions. The further compression of such an arrangement of azide ions could lead to the formation of a 'polymeric network' of nitrogen atoms, which is apparently realized in sodium azide.

Acknowledgments

We are grateful for financial support provided by the Deutsche Forschungsgemeinschaft (DFG) under grants ER 539/1-1, ER 539/2-1 and KL 636/11-1. TP would like to acknowledge the financial support of the Foundation for Polish Science as part of the KOLUMB Programme.

References

- [1] Fair H D and Walker R F 1977 *Energetic Materials* vol 1 (New York: Plenum)
- [2] Seel M and Kunz A B 1991 *Int. J. Quantum Chem.* **39** 149
- [3] Gordienko A B, Zhuravlev Y N and Poplavnoi A S 1996 *Phys. Status Solidi b* **198** 707
- [4] Gordienko A B and Poplavnoi A S 1997 *Phys. Status Solidi b* **202** 941
- [5] Younk E H and Kunz A B 1997 *Int. J. Quantum Chem.* **63** 615
- [6] Zhu W, Xiao J and Xiao H 2006 *Chem. Phys. Lett.* **422** 117
- [7] Eremets M I, Gavriiliuk A G, Trojan I A, Dzivenko D A and Boehler R 2004 *Nat. Mater.* **3** 558
- [8] Eremets M I, Hemley R J, Mao H K and Gregoryanz E 2001 *Nature* **411** 170
- [9] Eremets M I, Popov M Y, Trojan I A, Denisov V N, Boehler R and Hemley R J 2004 *J. Chem. Phys.* **120** 10618
- [10] Popov M 2005 *Phys. Lett. A* **334** 317
- [11] Pringle G E and Noakes D E 1968 *Acta Crystallogr. B* **24** 262
- [12] Iqbal Z 1973 *J. Chem. Phys.* **59** 1769
- [13] Hoth W and Pyl G 1929 *Angew. Chem.* **42** 888
- [14] Hofman-Bang N 1957 *Acta Chem. Scand.* **11** 581
- [15] Eremets M I 2003 *J. Raman Spectrosc.* **34** 515
- [16] Baer B J, Chang M E and Evans W J 2008 *J. Appl. Phys.* **104** 034504
- [17] Dewaele A, Loubeyre P and Mezouar M 2004 *Phys. Rev. B* **70** 094112
- [18] Spetzler H, Sammis C G and O'Connell R J 1972 *J. Phys. Chem. Solids* **33** 1727
- [19] Campbell I D and Coogan C K 1966 *J. Chem. Phys.* **44** 2075
- [20] Cruickshank D W J 1956 *Acta Crystallogr.* **9** 1005
- [21] Cahill J E and Leroi G E 1969 *J. Chem. Phys.* **51** 97